


Anomalous Hall effect in $\text{La}(\text{Fe}, \text{Co})_{13-x}\text{Si}_x$ compoundsDmitriy Yu. Karpenkov ^{*}*TU Darmstadt, Materials Science, Functional Materials, Alarich-Weiss-Strasse 16, 64287 Darmstadt, Germany;
National University of Science and Technology “MISIS,” 119049 Moscow, Russia;
and National Research South Ural State University, Chelyabinsk, 454080 Russia*

Konstantin P. Skokov, Iliya A. Radulov, and Oliver Gutfleisch

TU Darmstadt, Materials Science, Functional Materials, Alarich-Weiss-Strasse 16, 64287 Darmstadt, Germany

Jürgen Weischenberg and Hongbin Zhang

TU Darmstadt, Materials Science, Theory Magnetic Materials, Otto-Berndt-Strasse 3, 64287 Darmstadt, Germany

(Received 28 January 2019; revised manuscript received 19 August 2019; published 30 September 2019; corrected 9 December 2020)

We have measured the resistivity and Hall effect of $\text{La}(\text{Fe}, \text{Co})_{13-x}\text{Si}_x$ polycrystals in the temperature range of $100 \text{ K} < T < 340 \text{ K}$ and applied magnetic fields of up to 5 T. Detailed investigation combining experimental and theoretical means suggests that the anomalous Hall effect in $\text{La}(\text{Fe}, \text{Co}, \text{Si})_{13}$ originates mainly from the scattering independent intrinsic contributions, in turn, the anomalous Hall conductivity can be greatly enhanced with increasing Co doping concentration.

DOI: [10.1103/PhysRevB.100.094445](https://doi.org/10.1103/PhysRevB.100.094445)**I. INTRODUCTION**

The Hall effect, along with the electrical resistivity, is the key property used in the characterization of the fundamental electrical conduction in metals. In particular, the Hall effect in ferromagnets shows an “anomalous” term that is proportional to the magnetization of the material, in addition to the ordinary term which arises from the Lorentz force imposed on the carriers by the external magnetic fields. It is generally accepted that the skew scattering mechanism [1] in which spin-orbit coupling causes spin-polarized electrons to be scattered preferentially to one side by impurities, and side-jump (SJ) scattering [2] in which the trajectories of scattered electrons shift to one side at impurity sites because of spin-orbit coupling contribute extrinsically to the anomalous Hall effect (AHE). They are both asymmetric and arise from spin-orbit interactions of current carriers [3]. The intrinsic AHE [4], independent of the scattering mechanism, is attributed to the Berry-phase effect on conduction electrons [5–7], caused by carrier hopping in a noncollinear spin-splitting effective field produced by a spin-lattice background.

For materials with itinerant electron transitions (IETs) where the interplay between magnetism and charge conduction plays a crucial role [8,9], the study of the AHE can provide unique information about the evolution of the itinerant electronic structure upon IET. Indeed, the magnetization, magnetocaloric, and magnetovolume effects have been extensively studied for different IET materials, however, the transport properties associated with the metamagnetic transition require more detailed analysis, e.g., peculiar temperature and field dependencies of AHE can shed more light on the nature of the IETs.

$\text{La}(\text{Fe}, \text{Co})_{13-x}\text{Si}_x$ compounds exhibiting IETs are considered among the most promising candidate materials for applications as a working body in magnetic refrigerators [10–12]. They show a giant magnetocaloric effect which is due to the first-order field and thermally induced metamagnetic phase transition from a paramagnetic to a ferromagnetic state [13,14]. However, the fact that a maximum of the magnetocaloric effect is observed at low temperatures prevents the application of these compounds for room-temperature refrigeration. Still, a raise of the Curie temperature without significant loss of magnetization is possible by substitution of a part of Fe atoms with other magnetic transition metals and hydrogenation. It has been shown that the optimal effect can be obtained by substituting Co atoms for Fe [15–17]. The magnetic entropy change ΔS_m in the $\text{LaFe}_{10.98}\text{Co}_{0.22}\text{Si}_{1.8}$ compound at 242 K is $11.5 \text{ J kg}^{-1} \text{ K}^{-1}$ in an external magnetic field of 50 kOe. In the course of further investigations [15], it was found that the maximum value of ΔS_M for the $\text{LaFe}_{11.2}\text{Co}_{0.7}\text{Si}$ compound at 274 K (T_C) is $20.3 \text{ J kg}^{-1} \text{ K}^{-1}$ in a changing magnetic field of 0–50 kOe, which exceeds the value for Gd by two times and is almost comparable with $\text{Gd}_5\text{Si}_2\text{Ge}_2$ and $\text{MnFeP}_{0.45}\text{As}_{0.55}$.

Apart from their role as magnetocaloric materials, $\text{La}(\text{Fe}, \text{Co})_{13-x}\text{Si}_x$ compounds are also interesting because both magnetic and structural transitions lead to significant changes in their charge-carrier concentration and, subsequently, alter the scattering mechanisms, which can be detected by measuring their electron transport properties. In particular, the substitution of Fe atoms by Co atoms changes the order of phase transition from first to second. In this paper, we present a combined experimental and theoretical investigation of such transport properties by examining the Hall effect and the electrical resistance in $\text{La}(\text{Fe}, \text{Co})_{13-x}\text{Si}_x$ compounds. Furthermore, we studied the dependence of the AHE with

^{*}Corresponding author: karpenkov.dy@misis.ru

respect to the resistivity and the underlying mechanisms of the AHE, focusing on the role of phase transitions. Our efforts are helpful to deepen the understanding of such an important class of materials and highlight how a phase transition can change the relative strength of scattering mechanisms for transport properties.

This paper is structured as follows. In Sec. II, we describe our experimental approach and present our measured data. In Sec. III, we shortly recapitulate the basic theory of the anomalous Hall effect and explain its theoretical calculation from the Kubo-Středa formula in the framework of density functional theory and Wannier functions. In this context, we interpret our experimental findings by comparing them to the calculated values for the scattering-independent contributions to the transverse conductivity in LaFeSi. We conclude with a summary and outlook in Sec. IV.

II. EXPERIMENT

Polycrystalline $\text{La}(\text{Fe}, \text{Co})_{13-x}\text{Si}_x$ alloys were produced by Vacuumschmelze (Hanau, Germany). Detailed processing has been previously described in Ref. [18]. The $\text{LaFe}_{1.5}\text{Si}_{1.5}$ sample was prepared as described in Ref. [19]. Measurements of the magnetization, the electrical resistivity, and the Hall effect were carried out on the physical properties measurement system 14. The magnetotransport measurements were performed on bar-shaped samples with a typical size of $0.5 \times 1 \times 5 \text{ mm}^3$. We used a six-probe method to check for samples' homogeneity in both resistivity and Hall coefficient. The relative error obtained for the resistivity is about 0.1%; absolute values are determined to within 5%.

Hall effect measurement results for all samples are shown in Fig. 1. It is well known that the Hall resistance in ferromagnetic materials is generally represented as a sum of two terms,

$$\rho_H = R_0 B_z + 4\pi R_S M_z, \quad (1)$$

where the first one describes the ordinary Hall effect (OHE) due to the Lorentz force and the second one describes the AHE associated with the effect of the spin-orbit interaction. R_0 and R_S are OHE and AHE constants, respectively, M_z is the magnetization component along the z axis, and B_z is a component of the magnetic induction,

$$B_z = H_z + 4\pi M_z(1 - N_z), \quad (2)$$

where $0 < N_z < 1$ is the demagnetization factor.

Usually, three competing mechanisms of the AHE associated with the spin-orbit interaction are considered: the mechanism of Karplus-Luttinger (KL), otherwise referred to as the intrinsic contribution, the skew scattering mechanism, and the side-jump mechanism.

The mechanism of the KL has been proposed in Ref. [19]. It was shown that, in an ideal crystal lattice, if the spin of the electron interacts with its own spin-orbital motion (SOI), there is a linear amendment to the speed that causes AHE. In this case, the contribution to AHE does not depend on the impurity concentration, the type, and the size of the scattering potential. If the mechanism of KL is dominant, then it should lead to a quadratic dependence for any ferromagnets at all

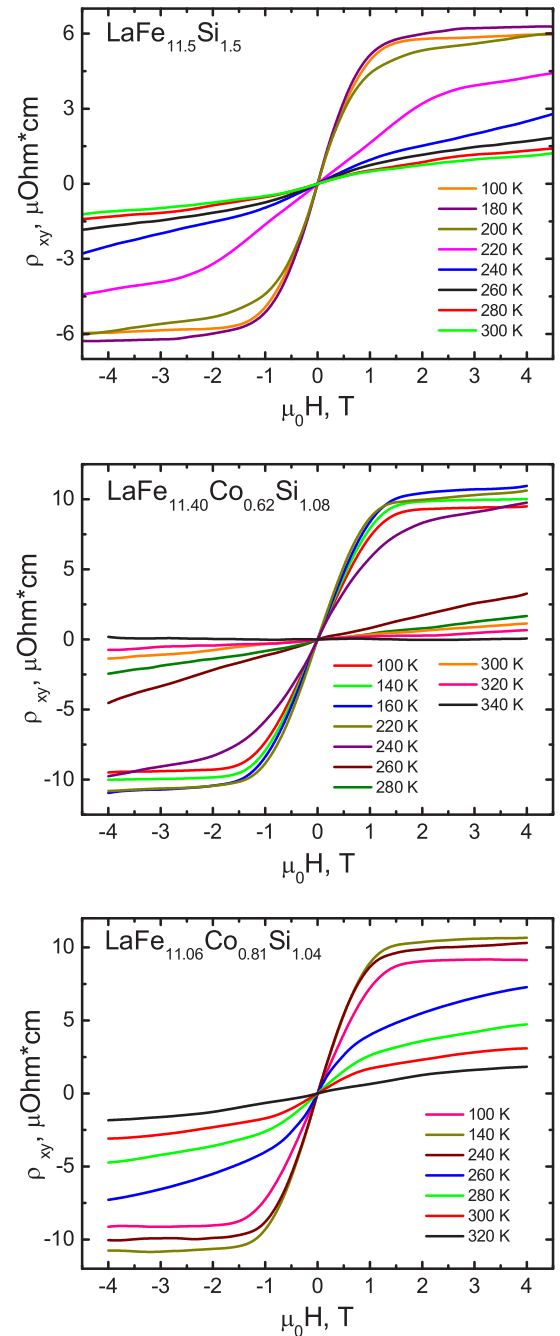


FIG. 1. Field dependence of Hall resistivity of $\text{LaFe}_{11.5}\text{Si}_{1.5}$ (top), $\text{LaFe}_{11.40}\text{Co}_{0.62}\text{Si}_{1.08}$ (middle), and $\text{LaFe}_{11.06}\text{Co}_{0.81}\text{Si}_{1.04}$ (bottom).

temperatures,

$$R_H \propto \rho_{int} = B\rho_{xx}^2. \quad (3)$$

The mechanism of the KL leaves out an important contribution suggested by Smit [1], who argued that the contribution of KL is fully compensated by other terms in the kinetic-energy solutions which are associated with scattering. To account for these effects, the mechanism of asymmetric scattering (skew scattering) was offered. The essence of this mechanism is that, in the presence of the SOI, the probability of electron scattering in opposite directions along with the y axis in the

direction of movement along the x axis becomes dependent on the direction of its spin along the z axis. According to the new scaling technique, proposed and approved by Tian *et al.* [20], the following equation is used:

$$R_H \propto \rho_{sk} = \alpha \rho_{xx0} + \beta \rho_{xx0}^2, \quad (4)$$

where ρ_{xx0} is the residual resistivity. The second term is smaller than the first and has an opposite sign. If the scattering is strong and the impurity concentration is not very small, then both terms may be of the same order of magnitude and have the same sign.

The third mechanism, proposed by Berger [2], is an abrupt change in the electrons trajectory in scattering by impurities due to the SOI. This mechanism is called a side-jump contribution. Like the KL mechanism, the side-jump mechanism does neither depend on the impurity concentration nor on the type and the size of the scattering potential, i.e., the value of the Hall coefficient is described by the relation,

$$R_H \propto \rho_{sj} = \beta \rho_{xx0}^2. \quad (5)$$

Thus, after combining of intrinsic and extrinsic contributions, we can write the final equation for anomalous Hall resistivity,

$$\rho_{xy} = \alpha \rho_{xx0} + \beta \rho_{xx0}^2 + B \rho_{xx}^2. \quad (6)$$

It should be mentioned that there are two possible interpretations of the term $\propto \rho_{xx0}^2$ in Eq. (6). The one is that it comes from the second-order contribution of the extrinsic skew scattering as predicted Crépieux and Bruno [21]. However, in Ref. [20], the authors suggested that the β term is presumably the long sought after the extrinsic side jump if the phonon contribution to the side jump is not relevant. Accordingly, if the experimentally measured off-diagonal resistivity ρ_{xy} is plotted against ρ_{xx} , the exponent in the scaling relations from Eq. (6) reveals which contribution to the AHE is important. In order to find the correct scaling behavior, the longitudinal resistivity ρ_{xx} has to be varied appropriately.

We first discuss the results from electrical resistivity measurements. Temperature dependencies of the electrical resistivity ρ_{xx} measured in the zero field in the cooling protocol are shown in Fig. 2(a). It can be seen that there are anomalies in the vicinity of the magnetic phase-transition temperature. Below the Curie point, the electrical resistance increases with increasing of temperature and has a form typical for ferromagnetic metal [22]. However, there is a sharp decrease in the resistance in a narrow range of T_C . It should be noted that the magnitude of the anomaly increases with rising of the Co content in the samples. Attempts to explain the observed behavior of the temperature dependence of the resistivity were made by de Gennes and Friedel [23]. They considered these anomalies in terms of spin fluctuations, although these authors failed to reproduce the sharpness of the anomaly. Using the same physical ideas, Fisher and Langer in Ref. [24] made great strides in this regard. If abnormalities observed in these compounds explained by low-order spin fluctuations near the critical point, in accordance with the Fischer and Langer model, sharp maximum can be expected above the Curie point. However, these do not occur for our samples. Perhaps, the model of Fisher and Langer is not suitable to explain the anomalies detected in the $\text{La}(\text{Fe}, \text{Co})_{13-x}\text{Si}_x$ compounds. Somewhat better agreement between theory and

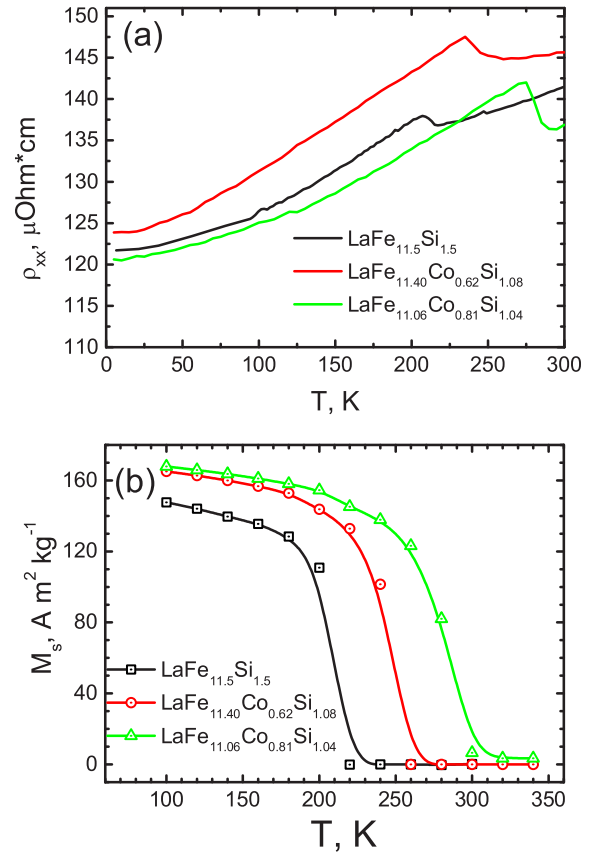


FIG. 2. Temperature dependencies of (a) longitudinal resistivity and (b) spontaneous magnetization.

experiment is observed in the model proposed by Kim [25], which predicted a sharp peak at the phase transition [26].

In $\text{La}(\text{Fe}, \text{Co})_{13-x}\text{Si}_x$ compounds, the magnetic phase transition is accompanied by a change in the lattice parameter. Therefore, it is considered that the change in the electron-phonon scattering at the phase transition may be responsible for reducing of the resistance in the paramagnetic phase. The sharp and significant change in the lattice parameter can affect the density of states near the Fermi level and, thus, influences the electron-phonon scattering.

Next, we have determined the dominant contributions to the AHE in these compounds. There are several scaling approaches of $\rho_{xy}(\rho_{xx})$ or $\sigma_{xy}(\sigma_{xx})$ dependences [20,27–31]. For this purpose, it is necessary to plot the Hall resistivity or Hall conductivity, measured in fields exceeding the saturation field, against the longitudinal resistivity (conductivity), as is shown in Fig. 3. Since in the paramagnetic state, an anomalous Hall effect cannot be observed, a sharp drop of the Hall resistance value occurs near the phase transition [see the inset in Fig. 3(a)]. Away from the Curie point, these dependences have no anomalies. Below, we compared the results of scaling, obtained by two different techniques, proposed by Tian *et al.* [20] and Onoda *et al.* [29].

In the first approach according to Eq. (6), the corresponding values of α , β , and B terms were estimated and summarized in Table I. The colored dashed curves in Fig. 3(a) are fitting results with Eq. (6). The values of intrinsic and extrinsic mechanism contributions to the total value of anomalous Hall

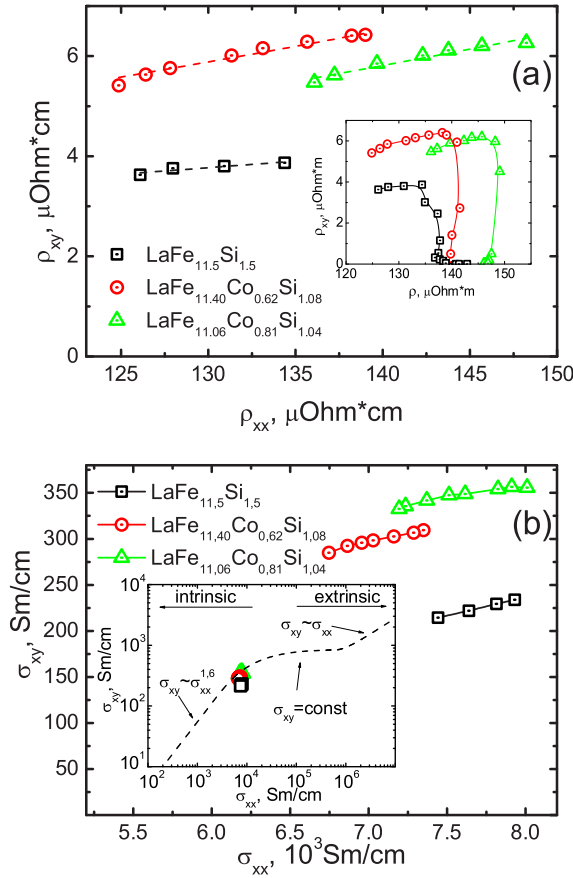


FIG. 3. (a) Dependency of the anomalous Hall resistivity ρ_{xy} on the longitudinal resistivity ρ_{xx} . The inset shows the plot of $\rho_{xy}(\rho_{xx})$ in the vicinity of phase transition. (b) Dependency of the anomalous Hall conductivity σ_{xy} on the longitudinal conductivity σ_{xx} . The inset shows the plot of $\sigma_{xy}(\sigma_{xx})$; the three dashed lines are $\sigma_{xy} = \sigma_{xx}^{1.6}$, $\sigma_{xy} = \text{const}$, and $\sigma_{xy} = \sigma_{xx}$ for the dirty, intermediate, and clean regimes, respectively [31].

resistivity calculated according to Eqs. (3)–(5) are listed in Table I. As shown in Table I for all samples, the contribution from the side-jump mechanism is negligibly small. With increasing in Co content, the intrinsic mechanism of AHE became dominant, its contribution raised from 50% to 80% and exhibit $\rho_{int} = 1.6$ and $\rho_{int} = 4.3 \mu\Omega \times \text{cm}$ for pure LaFe_{11.5}Si_{1.5} and LaFe_{11.06}Co_{0.81}Si_{1.04}, respectively.

The second approach is based on scaling of Hall conductivity dependence $\sigma_{xy}(\sigma_{xx})$ [see Fig. 3(b)]. The conductivity σ_{xx} was calculated as follows $\sigma_{xx} = 1/\rho_{xx}$, whereas $\sigma_{xy} = \rho_{xy}/\rho_{xx}^2$. According to the scaling technique of Onoda *et al.*, there are three regions with related values of the exponent in

TABLE I. Values of the fitting parameters with Eq. (6) and ρ_{sk} , ρ_{sj} , ρ_{int} , and ρ_{total} calculated for all samples.

Sample	α	β $\times 10^{-3}$	B	ρ_{sk}	ρ_{sj} ($\mu\Omega \times \text{cm}$)	ρ_{int}	ρ_{total}
LaFe _{11.5} Si _{1.5}	17.025	0	0.101	2.0	0	1.6	3.6
LaFe _{11.40} Co _{0.62} Si _{1.08}	10.411	0	0.231	1.9	0	3.7	5.6
LaFe _{11.06} Co _{0.81} Si _{1.04}	15.656	0	0.236	1.3	0	4.3	5.6

the scaling relation $\sigma_{xy} = \sigma_{xx}^X$ that reveals which contribution to the AHE is dominant: $X = 1.6$, $\sigma_{xy} = \text{const}$, and $X = 1$ for the dirty, intermediate, and clean regimes, respectively. As shown in the inset of Fig. 3(b), the value of conductivity for all samples lies on the edge of two regimes: dirty and intermediate. In the intermediate region with $\sigma_{xx} = 10^4$ – 10^6 S/cm, σ_{xy} is nearly constant, that corresponds to $\rho_{xy} \propto \rho_{xx}$ dependence. Hence, the extrinsic skew-scattering mechanism cannot contribute in this regime so much. Therefore, we can remark that σ_{xy} in the plateau region is dominated by the intrinsic mechanism of KL. Below $\sigma_{xx} = 10^4$ S/cm, in the dirty regime, the conductivity is completely determined by the intrinsic mechanism. It is worth noting that the absolute values of Hall conductivity upon Co substitution increases as is shown in Fig. 3(b).

Thus, both scaling techniques revealed, that is, the La(Fe, Si)₁₃ compounds where the dominant mechanism of AHE is the intrinsic one, moreover, its role increases with Co doping.

III. THEORY

To shed light on the experimentally observed AHE, we performed density functional theory (DFT) calculations on the scattering-independent (both the intrinsic and the SJ) contributions. Starting with the retarded Green's function in equilibrium and the Hamiltonian H of a general multiband noninteracting system in three spatial dimensions, we expand the self-energy of the system Σ_{eq} in powers of potential $V(\mathbf{r})$, which describes scattering at impurities. For a short-range scattering disorder model, scalar δ -correlated Gaussian disorder or δ -scattering uncorrelated disorder, the contribution to the self-energy which is of first order in $V(\mathbf{r})$ vanishes since one can assume that $\langle V(\mathbf{r}) \rangle = 0$ or else absorb $\langle V(\mathbf{r}) \rangle$ into the Hamiltonian, a procedure which results in a simple shift of the energy levels. Furthermore, inserting the expression for the self-energy within these simple disorder models into appropriate equations for the current densities derived following the Kubo-Středa formalism, rotating into eigenstate representation, and keeping only the leading order terms in the limit of vanishing disorder parameter \mathcal{V} , i.e., ignoring skew-scattering contributions, the scattering-independent part of the AHE conductivity may be written as $\sigma^{(0)} = \sigma^{int} + \sigma^{sj}$, where

$$\sigma_{ij}^{int} = \frac{e^2}{\hbar} \int \frac{d^3k}{(2\pi)^3} \text{Im} \sum_{n \neq m} (f_n - f_m) \frac{v_{nm,i}(\mathbf{k})v_{mn,j}(\mathbf{k})}{(\omega_n - \omega_m)^2} \quad (7)$$

can be recovered as the intrinsic contribution [6]. In this expression, indices n and m run over all bands with occupations f_n and f_m , respectively, $v_{nm,i}$ are the matrix elements of the velocity operator $\hat{v}_i = \partial_{\hbar k_i} \hat{H}$ and $\omega_n(\mathbf{k}) = \varepsilon_n(\mathbf{k})/\hbar$ with $\varepsilon_n(\mathbf{k})$ as band energies. The scattering-independent SJ contribution to conductivity $\sigma^{(0)}$ reads for inversion-symmetric systems,

$$\sigma_{ij}^{sj} = \frac{e^2}{\hbar} \sum_n \int \frac{d^3k}{(2\pi)^3} \text{Re} \text{Tr} \left\{ \delta(\varepsilon_F - \varepsilon_n) \frac{\gamma_c}{[\gamma_c]_{nm}} \times \left[S_n A_{k_i} (1 - S_n) \frac{\partial \varepsilon_n}{\partial k_j} - S_n A_{k_j} (1 - S_n) \frac{\partial \varepsilon_n}{\partial k_i} \right] \right\}. \quad (8)$$

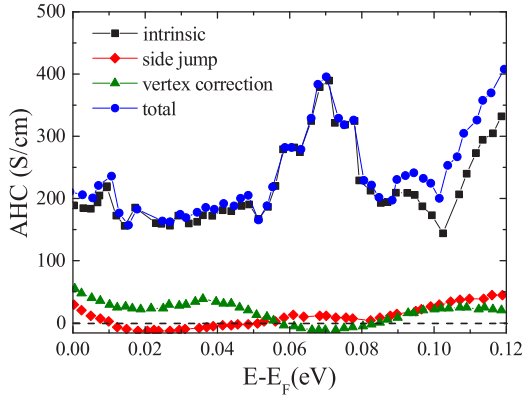


FIG. 4. Calculated scattering-independent anomalous Hall conductivity (AHC), including both the intrinsic and the side-jump contributions together with the vertex correction term.

Here, ε_F is the Fermi energy, and the imaginary part of the self-energy $\text{Im } \Sigma_{\text{eq}} = -\hbar\mathcal{V}\gamma$ is taken to be in the eigenstate representation, i.e., $\gamma_c = U^\dagger \gamma U$, with

$$\gamma = \frac{1}{2} \sum_n \int \frac{d^3k}{(2\pi)^2} U S_n U^\dagger \delta(\varepsilon_F - \varepsilon_n), \quad (9)$$

U as the \mathbf{k} -dependent unitary matrix that diagonalizes the Hamiltonian at point \mathbf{k} ,

$$[U^\dagger H(\mathbf{k})U]_{nm} = \varepsilon_n(\mathbf{k})\delta_{nm}, \quad (10)$$

S_n is a matrix that is diagonal in the band indices, $[S_n]_{ij} = \delta_{ij}\delta_m$, and the so-called Berry connection matrix is given by $A_{\mathbf{k}} = iU^\dagger \partial_{\mathbf{k}} U$ [32]. Not included in expression (8) are the vertex corrections, which vanish for an inversion-symmetric system in the Gaussian disorder model. However, note that, in contrast to the original formula as presented in Eq. (3) of Ref. [32], our expression for σ_{ij}^{sj} is manifestly antisymmetric. For the Rashba model, it reduces to the original form of Eq. (3) in Ref. [32]. It is important to note that the SJ contribution in the short-range disorder model, Eq. (8), is solely determined by the electronic structure of the pristine crystal and, thus, directly accessible by *ab initio* methods.

In practice, we replace the integrals in Eqs. (7) and (8) by a discrete sum over a finite number of k points in the Brillouin zone. To reduce the computational cost, we adopt the method of Wannier interpolation [33–35], which employs the description of the electronic structure in terms of maximally localized Wannier functions to evaluate Eqs. (7) and (8).

The electronic structure calculations of $\text{LaFe}_{11.5}\text{Si}_{1.5}$ were performed with the plane-wave method as implemented in the DFT code VASP [36] within the generalized gradient approximation as parametrized by Perdew-Burke-Ernzerhof [37,38]. We chose the energy cutoff E_{cut} of 500 eV and 16 k points for self-consistent calculations. The experimental

lattice constants are used. Spin-orbit coupling was included in the calculations in a second variation. For the Wannier interpolation, 384 Wannier functions on a k mesh of $6 \times 6 \times 8$ have been constructed.

The calculated values for the scattering-independent anomalous Hall conductivity are depicted in Fig. 4. In order to take the effect of Co doping into account, we employed the so-called rigid band approximation and calculated σ_{xy} as a function of the Fermi energy level. The change of 0.12 meV in Fig. 4 corresponds to a change in ~ 2.0 electrons, i.e., a Co doping of around 8%. It can be seen that, as the number of electrons is increased, i.e., as the Co concentration is increased, the value of the intrinsic contribution is nearly doubling from 200 S/cm up to 350 S/cm, whereas the value of the side-jump contribution and the associated vertex corrections remains small. The comparative analysis of DFT analysis and experimental data have shown applicability of proposed theoretical approach for the calculating of AHC for such a complex compound as $\text{La}(\text{Fe}, \text{Co}, \text{Si})_{13}$. Theoretically estimated values of the total anomalous Hall conductivity are in good agreement with the empiric investigation [see Fig. 3(b)]. Although the skew-scattering contributions were ignored, theoretically obtained values indicate the relative importance of the intrinsic mechanism, in accordance with experiment.

IV. CONCLUSION

In this paper, we investigated the electron transport properties of $\text{La}(\text{Fe}_{1-x}\text{Co}_x)_{13-y}\text{Si}_y$ compounds. We have measured the resistivity and Hall effect of $\text{La}(\text{Fe}_{1-x}\text{Co}_x)_{13-y}\text{Si}_y$ polycrystals in the temperature range of $100 < T < 340$ K and applied magnetic fields of up to 5 T. It was found that the temperature dependence of longitudinal resistance has anomalies near the Curie temperature that is explained by the change in the electron-phonon scattering at the phase transition. The sharp and significant change in the lattice parameter can affect the density of states near the Fermi level and, thus, influence the electron-phonon scattering. The anomalous Hall effect is large and varies quite linearly with the longitudinal resistivity ρ_{xx} . AHE in these compounds is mostly determined by the contribution of the intrinsic mechanism. With increasing of the Co concentration, the value of the intrinsic contribution increases by more than 50%.

ACKNOWLEDGMENTS

This work was supported by the DFG (Grant No. SPP 1599) and by the European Research Council (ERC) under the European Unions Horizon 2020 research and innovation programme (Grant No. 743116 project Cool Innov). D.Y.K. gratefully acknowledges the financial support of the Ministry of Science and Higher Education of the Russian Federation in the framework of Increase Competitiveness Program of MISIS (Grant No. P02 2017-2-6) and the grant from RSF No. 18-42-06201.

[1] J. Smit, The spontaneous Hall effect in ferromagnetics I, *Physica* **21**, 877 (1955).

[2] L. Berger, Side-jump mechanism for the Hall effect of ferromagnets, *Phys. Rev. B* **2**, 4559 (1970).

- [3] N. Nagaosa, J. Sinova, S. Onoda, A. H. MacDonald, and N. P. Ong, Anomalous Hall effect, *Rev. Mod. Phys.* **82**, 1539 (2010).
- [4] R. Karplus and J. M. Luttinger, Hall effect in ferromagnetics, *Phys. Rev.* **95**, 1154 (1954).
- [5] T. Jungwirth, Q. Niu, and A. H. MacDonald, Anomalous Hall Effect in Ferromagnetic Semiconductors, *Phys. Rev. Lett.* **88**, 207208 (2002).
- [6] Y. Yao, L. Kleinman, A. H. MacDonald, J. Sinova, T. Jungwirth, D.-s. Wang, E. Wang, and Q. Niu, First Principles Calculation of Anomalous Hall Conductivity in Ferromagnetic bcc Fe, *Phys. Rev. Lett.* **92**, 037204 (2004).
- [7] R. Mathieu, A. Asamitsu, H. Yamada, K. S. Takahashi, M. Kawasaki, Z. Fang, N. Nagaosa, and Y. Tokura, Scaling of the Anomalous Hall Effect in $\text{Sr}_{1-x}\text{Ca}_x\text{RuO}_3$, *Phys. Rev. Lett.* **93**, 016602 (2004).
- [8] M. Shimizu, Itinerant electron metamagnetism, *J. Phys.* **43**, 155 (1982).
- [9] H. Yamada, Metamagnetic transition and susceptibility maximum in an itinerant-electron system, *Phys. Rev. B* **47**, 11211 (1993).
- [10] J. Liu, J. Moore, K. Skokov, M. Krautz, K. Löwe, A. Barcza, M. Katter, and O. Gutfleisch, Exploring $\text{La}(\text{Fe}, \text{Si})_{13}$ -based magnetic refrigerants towards application, *Scr. Mater.* **67**, 584 (2012).
- [11] K. Morrison, K. Sandeman, L. Cohen, C. Sasso, V. Basso, A. Barcza, M. Katter, J. Moore, K. Skokov, and O. Gutfleisch, Evaluation of the reliability of the measurement of key magnetocaloric properties: A round robin study of $\text{La}(\text{Fe}, \text{Si}, \text{Mn})\text{H}_3$ conducted by the SSEEC consortium of european laboratories, *Int. J. Refrig.* **35**, 1528 (2012).
- [12] J. D. Moore, D. Klemm, D. Lindackers, S. Grasmann, R. Träger, J. Eckert, L. Löber, S. Scudino, M. Katter, A. Barcza, K. P. Skokov, and O. Gutfleisch, Selective laser melting of $\text{La}(\text{Fe}, \text{Co}, \text{Si})_{13}$ geometries for magnetic refrigeration, *J. Appl. Phys.* **114**, 043907 (2013).
- [13] S. Fujieda, A. Fujita, and K. Fukamichi, Large magnetocaloric effect in $\text{La}(\text{Fe}_x\text{Si}_{1-x})_{13}$ itinerant-electron metamagnetic compounds, *Appl. Phys. Lett.* **81**, 1276 (2002).
- [14] O. Gutfleisch, A. Yan, and K.-H. Müller, Large magnetocaloric effect in melt-spun $\text{LaFe}_{13-x}\text{Si}_x$, *J. Appl. Phys.* **97**, 10M305 (2005).
- [15] F. X. Hu, J. Gao, X. L. Qian, M. Ilyn, A. M. Tishin, J. R. Sun, and B. G. Shen, Magnetocaloric effect in itinerant electron metamagnetic systems $\text{La}(\text{Fe}_{1-x}\text{Co}_x)_{11.9}\text{Si}_{1.1}$, *J. Appl. Phys.* **97**, 10M303 (2005).
- [16] K. P. Skokov, A. Y. Karpenkov, D. Y. Karpenkov, and O. Gutfleisch, The maximal cooling power of magnetic and thermoelectric refrigerators with $\text{La}(\text{FeCoSi})_{13}$ alloys, *J. Appl. Phys.* **113**, 17A945 (2013).
- [17] M. G. Zavareh, Y. Skourski, K. P. Skokov, D. Y. Karpenkov, L. Zvyagina, A. Waske, D. Haskel, M. Zhernenkov, J. Wosnitzer, and O. Gutfleisch, Direct Measurement of the Magnetocaloric Effect in $\text{La}(\text{Fe}, \text{Si}, \text{Co})_{13}$ Compounds in Pulsed Magnetic Fields, *Phys. Rev. Appl.* **8**, 014037 (2017).
- [18] M. Katter, V. Zellmann, G. Reppel, and K. Uestuener, Magnetocaloric properties of $\text{La}(\text{Fe}, \text{Co}, \text{Si})_{13}$ bulk material prepared by powder metallurgy, *IEEE Trans. Magn.* **44**, 3044 (2008).
- [19] J. Liu, M. Krautz, K. Skokov, T. G. Woodcock, and O. Gutfleisch, Systematic study of the microstructure, entropy change and adiabatic temperature change in optimized LaFeSi alloys, *Acta Mater.* **59**, 3602 (2011).
- [20] Y. Tian, L. Ye, and X. Jin, Proper Scaling of the Anomalous Hall Effect, *Phys. Rev. Lett.* **103**, 087206 (2009).
- [21] A. Crépieux and P. Bruno, Theory of the anomalous Hall effect from the Kubo formula and the Dirac equation, *Phys. Rev. B* **64**, 014416 (2001).
- [22] T. Kasuya, Electrical resistance of ferromagnetic metals, *Prog. Theor. Phys.* **16**, 58 (1956).
- [23] P. D. Gennes and J. Friedel, Anomalies de résistivité dans certains métaux magnétiques, *J. Phys. Chem. Solids* **4**, 71 (1958).
- [24] M. E. Fisher and J. S. Langer, Resistive Anomalies at Magnetic Critical Points, *Phys. Rev. Lett.* **20**, 665 (1968).
- [25] D.-J. Kim, Electrical resistance in ferromagnetic metals and dilute alloys near the Curie temperature, *Prog. Theor. Phys.* **31**, 921 (1964).
- [26] M. P. Kawatra, S. Skalski, J. A. Mydosh, and J. L. Budnick, Effect of the Molecular Field on the Electrical Resistivity Near a Magnetic Transition: GdNi_{14} , *Phys. Rev. Lett.* **23**, 83 (1969).
- [27] C. Zeng, Y. Yao, Q. Niu, and H. H. Weitering, Linear Magnetization Dependence of the Intrinsic Anomalous Hall Effect, *Phys. Rev. Lett.* **96**, 037204 (2006).
- [28] B. C. Sales, R. Jin, and D. Mandrus, Orientation dependence of the anomalous Hall resistivity in single crystals of $\text{Yb}_{14}\text{MnSb}_{11}$, *Phys. Rev. B* **77**, 024409 (2008).
- [29] S. Onoda, N. Sugimoto, and N. Nagaosa, Intrinsic Versus Extrinsic Anomalous Hall Effect in Ferromagnets, *Phys. Rev. Lett.* **97**, 126602 (2006).
- [30] D. Hou, G. Su, Y. Tian, X. Jin, S. A. Yang, and Q. Niu, Multivariable Scaling for the Anomalous Hall Effect, *Phys. Rev. Lett.* **114**, 217203 (2015).
- [31] T. Miyasato, N. Abe, T. Fujii, A. Asamitsu, S. Onoda, Y. Onose, N. Nagaosa, and Y. Tokura, Crossover Behavior of the Anomalous Hall Effect and Anomalous Nernst Effect in Itinerant Ferromagnets, *Phys. Rev. Lett.* **99**, 086602 (2007).
- [32] A. A. Kovalev, J. Sinova, and Y. Tserkovnyak, Anomalous Hall Effect in Disordered Multiband Metals, *Phys. Rev. Lett.* **105**, 036601 (2010).
- [33] X. Wang, J. R. Yates, I. Souza, and D. Vanderbilt, *Ab initio* calculation of the anomalous Hall conductivity by Wannier interpolation, *Phys. Rev. B* **74**, 195118 (2006).
- [34] X. Wang, J. R. Yates, I. Souza, and D. Vanderbilt, Erratum: *Ab initio* calculation of the anomalous Hall conductivity by Wannier interpolation, *Phys. Rev. B* **76**, 169902(E) (2007).
- [35] J. R. Yates, X. Wang, D. Vanderbilt, and I. Souza, Spectral and Fermi surface properties from Wannier interpolation, *Phys. Rev. B* **75**, 195121 (2007).
- [36] VASP documentation (2009).
- [37] J. P. Perdew, K. Burke, and M. Ernzerhof, Generalized Gradient Approximation Made Simple, *Phys. Rev. Lett.* **77**, 3865 (1996).
- [38] J. P. Perdew, K. Burke, and M. Ernzerhof, Erratum: Generalized Gradient Approximation Made Simple, *Phys. Rev. Lett.* **78**, 1396 (1997).

Correction: A third affiliation has been added for the first author.